Conversion of an inactive cardiac dihydropyridine receptor II-III loop segment into forms that activate skeletal ryanodine receptors

Xinsheng Zhu, Georgina Gurrola, Ming Tao Jiang, Jeffery W. Walker, Hector H. Valdivia*

Department of Physiology, University of Wisconsin Medical School, 1300 University Ave., Madison, WI 53706, USA

Abstract A 25 amino acid segment (Glu^{666}–Pro^{691}) of the II-III loop of the α_1 subunit of the skeletal dihydropyridine receptor, but not the corresponding cardiac segment (Asp^{788}–Pro^{814}), activates skeletal ryanodine receptors. To identify the structural domains responsible for activation of skeletal ryanodine receptors, we systematically replaced amino acids of the cardiac II-III loop with their skeletal counterparts. A cluster of five basic residues of the skeletal II-III loop (^{681}RKRRK^{685}) was indispensable for activation of skeletal ryanodine receptors. In the cardiac segment, a negatively charged residue (Glu^{804}) appears to diminish the electrostatic potential created by this basic cluster. In addition, Glu^{800} in the group of negatively charged residues ^{798}EEEEE^{802} of the cardiac II-III loop may serve to prevent the binding of the activation domain.

© 1999 Federation of European Biochemical Societies.

Key words: Dihydropyridine receptor; Ryanodine receptor; Excitation-contraction coupling; Sarcoplasmic reticulum; Synthetic peptide

1. Introduction

Excitation-contraction coupling (E-C coupling), the series of events in cardiac and skeletal muscle by which depolarization of the external membrane evokes a mechanical contraction, is largely dependent on molecular interactions between the dihydropyridine receptor (DHPR) of the external membrane and the Ca^{2+} release channel/ryanodine receptor (RyR) of the sarcoplasmic reticulum (SR). In the heart, a small influx of Ca^{2+} through DHPRs triggers the opening of RyRs [1,2]. In skeletal muscle, external Ca^{2+} is not required for Ca^{2+} release [3]. Instead, a direct physical interaction between the DHPR and the RyR is thought to mediate E-C coupling [4,5].

DHPR and RyR subtypes dictate the different E-C coupling modalities. In skeletal muscle paralyzed by the absence of the α_1 subunit of the DHPR, expression of the cardiac α_1 subunit results in Ca^{2+}-dependent ('cardiac-type') E-C coupling. Conversely, expression of a chimeric α_1 subunit that is entirely cardiac except for the cytoplasmic loop between repeats II and III (the II-III loop) restores voltage-dependent ('skeletal-type') E-C coupling [6]. In transgenic mice that lack skeletal RyR (RyR1), transfection of myoblasts with RyR1 restores the voltage-dependent Ca^{2+} release, however, transfection with cardiac RyR (RyR2) requires external

Ca^{2+} for SR Ca^{2+} release [7]. Thus, specific protein-protein interactions between the skeletal DHPR and RyR1 are responsible for coupling membrane depolarization to Ca^{2+} release. The skeletal II-III loop plays a prominent role in these interactions. Indeed, the skeletal II-III loop activates purified RyR1 [8] and a 20 amino acid segment of the skeletal II-III loop (Thr^{671}–Leu^{690}), but not the corresponding cardiac segment, induces Ca^{2+} release from SR vesicles [9]. In the present report, we compared an active segment of the skeletal II-III loop with its inactive cardiac counterpart to define the structural elements that support, and those that prevent, the activation of RyR1.

2. Materials and methods

2.1. Preparation of SR microsomes

Skeletal and cardiac SR-enriched microsomes were isolated from rabbit white back and leg muscle and pig hearts, respectively, as previously described [10]. Microsomes from the last centrifugation were suspended in 0.3 M sucrose, 0.1 M KCl and 5 mM Na-PIPES (pH 7.2)

2.2. Synthesis and modelling of peptides

Peptides were synthesized by the solid phase methodology with Fmoc (N-(9-fluorenyl)methoxycarbonyl) amino acids in an Applied Byosystems peptide synthesizer (Model 432A), as described [11]. Peptides were cleaved and deprotected with 95% trifluoroacetic acid and purified in a reverse-phase C_{18} HPLC column, also as described in [11]. The structure and purity of the peptides were confirmed by mass spectrometry. Peptides were quantified in a Model 8452A Hewlett-Packard Spectrophotometer using the expression 1 $A_{214 \text{ nm}} = 20$ mg peptide/ml. Structural models were obtained using Insight II Discover software from Biosym Technologies (San Diego, CA, USA), running on a Silicon Graphics Octane RS10000 Workstation. Models were built by the Biopolymer module of Insight II on the basis of the amino acid sequence propensity to form α-helix, random coil and β-sheet structures, as determined by the programs Agadir [12] and Gor IV [13] in the Expert Protein Analysis System (ExPASy) website (http://www.expasy.ch/www/tools.html). The structures were energy minimized using the Discover force field. 500 steps of minimization were performed using the steepest descent algorithm method until a root mean square deviation of 0.001 was obtained.

2.3. [³H]ryanodine binding assay

[³H]ryanodine (7 nM) was incubated for 90 min at 36°C with 40–50 μg of rabbit skeletal or pig cardiac SR vesicles in 0.1 ml of medium containing 0.2 M KCl, 10 μM $CaCl_2$ and 10 mM Na-HEPES (pH 7.2) in the absence and presence of peptides. Free and bound ligands were separated by rapid filtration through Whatman GF/B glass fiber filters, as described [11,14].

2.4. Planar bilayer technique

Rabbit skeletal RyRs were reconstituted into Muller-Rudin planar lipid bilayers as described previously [14,15]. Single channel data were collected at steady voltages (+35 mV) for 2 min in symmetrical 300 mM cesium methanesulfonate and 10 mM Na-HEPES (pH 7.2). Contaminant Ca^{2+} ions (∼5–7 μM free Ca^{2+} as assessed by a calibration curve) served to activate RyRs. Signals were digitized at 4 kHz and analyzed after filtering with a low-pass 8-pole Bessel filter at a sam-

---

*Corresponding author. Fax: (1) (608) 265 5512.
E-mail: valdivia@physiology.wisc.edu

pling frequency of 1.5 kHz. Date acquisition and analysis were done with Axon instruments software and hardware (pClamp V6.03, Digidata 200 AD/DA interface).

2.5. Spectrophotometric Ca^{2+} release assay

Skeletal SR vesicles (~50 μg of protein) were mixed in a 1 ml solution containing 95 mM KCl, 7.5 mM Na-pyrophosphate, 250 μM antipyrylazo III, 1.5 mM MgATP, 25 μg/mg creatine phosphokinase, 5 mM phosphocreatine and 20 mM K-MOPS, (pH 7.0). The solution was placed in a cuvette, thermostated at 37°C and allowed to equilibrate for 2 min. Changes in free Ca^{2+} were monitored by changes in the absorbance of antipyrylazo at 710 nm and subtraction of the absorbance at 790 nm, at 1 s intervals, using a diode array spectrophotometer (Hewlett Packard Model 8452A). Vesicles were actively loaded with $CaCl_2$ until levels close to the filling capacity (~2 μmol of total Ca^{2+}/mg protein, usually four additions of 10 nmol of $CaCl_2$). The absorbance signals were calibrated by addition of a known amount of Ca^{2+} to the complete transport mixture in the presence of the Ca^{2+} ionophore A23187 to prevent Ca^{2+} accumulation.

3. Results and discussion

3.1. The effect of cardiac and skeletal II-III loop segments on $[^3H]$ryanodine binding

Earlier work by El-Hayek et al. [9] suggested that the capacity of the 138 amino acid II-III loop of the skeletal DHPR to activate RyR1 could be attributed to a 20 amino acid segment encompassing the sequence Thr^{671}–Leu^{690}. We synthesized the corresponding segment of the cardiac II-III loop to test its capacity to activate RyRs. Fig. 1A shows that, with the exception of a few amino acids (gray boxes), the 25 amino acid peptide of the cardiac sequence (peptide Car) is highly homologous to the skeletal II-III loop segment (peptide Ske) that activates RyR1. However, while peptide Ske stimulates $[^3H]$ryanodine binding to skeletal SR with a half-maximal effective concentration $(ED_{50}) = 0.8$ μM, peptide Car stimulates binding only marginally (Fig. 1B). The stimulating effect of peptide Ske cannot be attributed to the peptide mass or net electrical charge because a scrambled peptide Ske (a synthetic peptide with amino an acid composition identical to peptide Ske but in a random sequence) lacks the capacity to activate $[^3H]$ryanodine binding (Fig. 1B). Thus, the stimulating effect of peptide Ske seems to require a defined amino acid sequence. Accordingly, amino acid substitutions in peptide Car that yield a peptide more similar to peptide Ske should gradually enhance its potential to activate RyRs.

To define the minimal structural elements that support or prevent activation of RyR1 by peptide segments of the II-III loop, we synthesized truncated forms of peptide Car and full-length versions of the same with amino acid substitutions in one or more positions to resemble peptide Ske (Fig. 1A). Two regions of electrically charged amino acids in peptide Car are notoriously divergent from those in peptide Ske and were therefore targeted for mutations. Region 1 (Fig. 1A) is of high electrostatic potential in peptide Car as it is formed of five consecutive glutamate residues (^{798}EEEEE^{802}). Conversely, region 2 is a cluster of five basic residues in peptide Ske (^{681}RKRRK^{685}), a cluster that is interrupted by the negatively charged residue glutamate in peptide Car (^{803}KERKK^{807}). This cluster of five basic amino acids in peptide Ske is believed to be important for activation of RyR1 [16]. For instance, replacing Arg^{684} with glutamate renders peptide Ske inactive [16]. The participation of other regions of peptide Ske in the activation of RyRs remains uncertain.
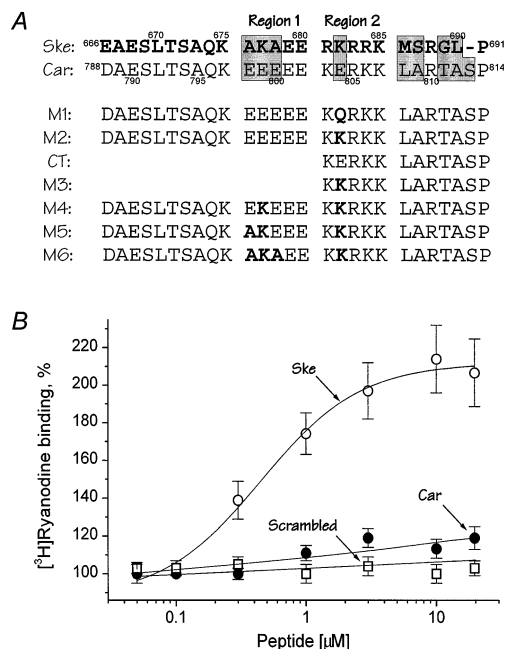

Fig. 1. Synthetic peptides used in this study and the effect on $[^3H]$ryanodine binding. (A) Amino acid sequences (in one letter code) of synthetic peptides corresponding to skeletal (Ske) and cardiac (Car) segments of the II-III loop and different mutants (M1–M6). The amino acid sequences (but not the synthetic peptides) have been arbitrarily broken in four groups to facilitate analysis. Shaded areas indicate a lack of homology between peptides Ske and Car. Bold letters in peptides M1–M6 indicate the mutated residues. (B) The effect of peptides Ske, Car and a scrambled peptide Ske (RLKSQKMRATGKAERARSEK) on $[^3H]$ryanodine binding to skeletal SR. The binding assay was carried out as described in Section 2. Specific binding in the absence of peptides (control, 100%) was 0.33 ± 0.08 pmol/mg protein.

We therefore designed several peptides to investigate the role of these structural domains separately. Peptides M1 and M2 were designed to test the hypothesis that the disruption of the cluster of basic amino acids in region 2 was the only structural basis for the lack of effect of peptide Car. The other peptides were designed to investigate the role of region 1 and the conserved first 12 amino acids. Peptides CT and M3 are truncated forms of peptide Car that lack region 1 and the first 12 amino acids. Peptides M4, M5 and M6 are full-length versions of peptide Car with a skeletal-like region 2 and mutations in region 1.

We first investigated the role of the cluster of five basic amino acids. Fig. 2A shows that the truncated peptide M3, but not peptides M1, M2 and CT, was capable of stimulating $[^3H]$ryanodine binding to skeletal SR in a substantial manner. Peptide M3 had an $ED_{50} = 10$ μM and increased binding to the same extent as peptide Ske ($212 \pm 18\%$ and $210 \pm 10\%$, respectively, $n = 4$). The other mutated peptides were without an effect at concentrations up to 100 μM. The lack of effect by peptide CT was not surprising given that its cluster of basic residues is, like in peptide Car, disrupted by glutamate. However, peptides M1 and M2 do not contain the negatively charged residue and in fact, M2 displays the continuous cluster of five basic residues. Since the active peptide M3 is identical to the last twelve amino acids of the inactive peptide M2, a plausible interpretation of these results is that the first half of peptide M2, particularly its region 1, prevented the activa-

tion of RyR1. We thus tested the role of region 1 in the next experimental series.

We synthesized peptides M4, M5 and M6, which carry one or more mutations in region 1 (Fig. 1A). Since the above results suggested that the cluster of five basic residues was essential for activation, all three peptides were designed to contain that structural motif. Fig. 2B shows that peptide M6, but not peptides M4 and M5, stimulated [³H]ryanodine binding significantly. Although peptides M4 and M5 carry one and two substitutions, respectively, that eliminate an equal number of negative electrical charges in region 2, they were unable to increase [³H]ryanodine binding. Only peptide M6, whose regions 1 and 2 are essentially identical to peptide Ske, was capable of increasing binding, albeit to a maximum (170 ± 10%, $n = 4$) and with a potency ($ED_{50} = 10.5$ μM), lower than the latter. Taken together, the results of Fig. 2A and B suggest that one or more amino acids in the cluster of five basic residues is indispensable for activation of [³H]ryanodine binding to RyR1. In peptide Car, Glu^{804} appears to diminish the electrostatic potential created by this basic cluster. In addition, the group of negatively charged residues ($^{798}EEEEE^{802}$) may serve as an inhibitory domain to prevent the binding of the activation domain. However, the proposed interaction appears to involve more than these two clusters of charged residues because their conversion to a skeletal-like sequence in peptide Car does not yield a peptide as effective as peptide Ske. Based on previous work, Ser^{687} of the skeletal II-III loop appears to be important for activation of RyRs [16,17]. In peptide M6, Ser^{687} corresponds to Ala^{809}, a residue similar to Ser, except for the lack of the hydroxyl group in the β-carbon. It is therefore likely that the reduced efficacy of peptide M6 is at least partly due to the absence of the hydroxyl group contributed by Ser^{687}.

In RyR1 knock-out (dyspedic) mice, transfection of skeletal myoblasts with cDNA encoding RyR1 restores the voltage-dependent ('skeletal-type') Ca^{2+} release, however, myotubes transfected with RyR2 require external Ca^{2+} for Ca^{2+} release [7]. This suggests that the structural domain of RyR1, capable of coupling the membrane voltage to Ca^{2+} release, is absent in RyR2 [18]. Fig. 2C shows that, at concentrations up to 100 μM, none of the peptides, including peptide Ske, were capable of increasing [³H]ryanodine binding to RyR2. Thus, the effect of the peptides appears to be specific for RyR1. The results are compatible with the involvement of specific RyR subtypes to elicit the two different modalities of E-C coupling.

3.2. Functional effects of active peptides M3 and M6

To determine whether the increase of [³H]ryanodine binding to skeletal SR by peptides M3 and M6 (Fig. 2A and B) had a functional correlation, we tested their effect in Ca^{2+} release experiments and on single RyR reconstituted in lipid bilayers. Fig. 3 shows that peptides M3 (B) and M6 (D) elicited Ca^{2+} release from actively loaded skeletal SR vesicles in a dose-dependent manner. Addition of 1 μM peptide M3 or M6 to the incubation reaction released ≥65% and 50%, respectively, of the Ca^{2+} trapped in the SR vesicles. The effect of the peptides was blocked by ruthenium red (not shown), consistent with Ca^{2+} release occurring by RyRs. Fig. 3 also shows that 0.1 and 0.5 μM of peptide M3 (A) or the same concentrations of peptide M6 (C) added to the *cis* (cytoplasmic) side of RyR1 induced the appearance of subconductance states. The latter had at least two current amplitude values. In one
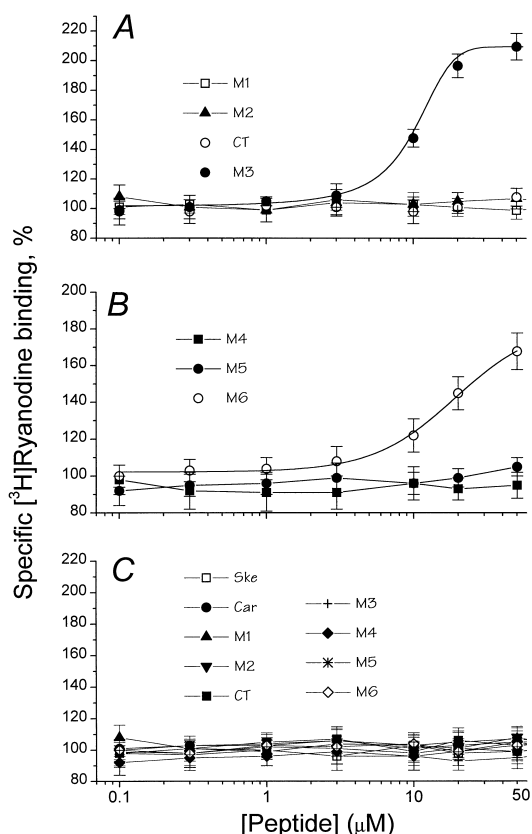

Fig. 2. Activation of [³H]ryanodine binding by selected peptides. Binding of 7 nM [³H]ryanodine to skeletal SR (A and B) and to cardiac SR (C) was conducted in the absence (control, 100%) or the presence of indicated concentrations of synthetic peptides, as described in Section 2. Specific binding to skeletal and cardiac SR was 0.55 and 0.17 pmol/mg protein, respectively. Data points represent the mean ± S.D. of $n = 4$ independent experiments.

case, openings were temporarily stable in a subconductance state corresponding to ∼3/4 of the full conductance level (first trace after addition of peptide M3). In the second and most frequent case, the subconductance state corresponded to ∼1/4 of the full conductance level. In both cases, current transitions from modified to normal amplitude levels were frequent. Although of a small amplitude, both types of subconductance states displayed a mean open time that was > 50-fold longer than that of unmodified channels. The ion flow would therefore be expected to be greater for a peptide M3- or peptide M6-modified channel despite its lower conductance. This effect may explain the Ca^{2+} releasing properties of the peptides. Hence, the capacity of peptides M3 and M6 to increase [³H]ryanodine binding appears to be the result of an increase in the overall activity of the channel. In support of this notion, peptide Ske evoked similar functional effects on RyR1 [16], but the inactive peptides Car and M2 did not (not shown).

3.3. Structural models of the skeletal and cardiac II-III loop peptides

To visualize more integrally the spatial arrangement of the putative binding domains, we created a three-dimensional model of peptides Ske and Car based on the propensity of their amino acid sequence to form α-helix, random coil and β-sheet strands. The model (Fig. 4) recapitulates the main find-

ings of this study and provides a structural framework to rationalize the activity (or lack thereof) of native and mutant peptides. To construct the model, we used two different algorithms (Agadir [12] and Gor IV [13], see Section 2) that predict helix/coil/β-sheet transitions and short range interactions in monomeric peptides under defined conditions of pH, temperature and ionic strength. In small and highly hydrophilic peptides such as peptides Ske and Car, this is relatively straightforward and, indeed, both algorithms yielded essentially identical results. The amino-termini of peptides Ske and Car ([666]EAESL- and [788]DAESL-, respectively), as well as their carboxyl-termini (-SRGLP[691] and -RTASP[814], respectively), lack propensity to form ordered secondary structures and are therefore assigned as random coil. In the carbon backbone representation (Fig. 4, left), they appear as thin threads extending outward from the well-ordered central core of the peptides. Although the model provided in Fig. 4 represents the structural conformation most thermodynamically favored, the amino- and carboxyl-termini of both peptides underwent major spatial transitions during energy minimization, suggesting that these segments may adopt several arrangements in relation to the central core. The central amino acids [671]TSAQKA[676] and [793]TSAQKE[798] of peptides Ske and Car, respectively, have a high probability ($\geq 90\%$) of forming α-helix and so do the neighboring sequences [679]EERKRRKM[686] and [801]EEKERKKLA[809] of peptide Ske and Car, respectively. These two sets of α-helices appear as thick ribbons in the backbone representation of the peptides, joined by thin threads representing two randomly coiled residues ([677]KA[678] and [799]EE[800], respectively).

The spacefill model (Fig. 4, middle) indicates the spatial orientation of all atoms of the amino acid residues forming the carbon backbone. A conspicuous difference between peptides Ske and Car is that in the former peptide, there is a cluster of positively charged residues aligned towards the same side of the molecule. These residues are outlined in color in Fig. 4, right, and correspond to Lys[677], Arg[681], Lys[682], Arg[684] and Lys[685]. Not surprisingly, most of these positively charged residues are found in region 2, except for Lys[677], which is the second residue of region 1. That Lys[677] contributes to the cluster of basic residues is counter-intuitive-based on the linear sequence, but is possible because in an α-helix, amino acids spaced three and four apart in the linear sequence are spatially close to one another. Each residue is related to the next one by a 100° rotation (or 3.6 residues per turn of α-helix) and residues two apart in the linear sequence are on opposite sides of the helix. This explains why not all basic residues of region 2 contribute to the formation of this structural domain. In sharp contrast, the corresponding region of peptide Car is composed of basic (Arg[805] and Lys[807]), hydrophobic (Leu[808]) and negatively charged (Glu[800] and Glu[804]) residues (Fig. 4, right). Since mutations in this structural domain determine the activity of peptides Ske and Car, we postulate that residues within it are part of the active binding site. Superposing these structural domains reveals that Lys[682] and Arg[684] of peptide Ske correspond to Arg[805] and Lys[807] of peptide Car. Because both pairs of residues are of the same electrical charge, they probably would favor the binding of peptide Car to RyRs. However, Glu[800] and Glu[804] of peptide Car contribute electrical charges of an opposite sign from residues that in peptide Ske appear favorable for activation of RyRs (Lys[677] and Arg[681]). Supporting the adverse role of
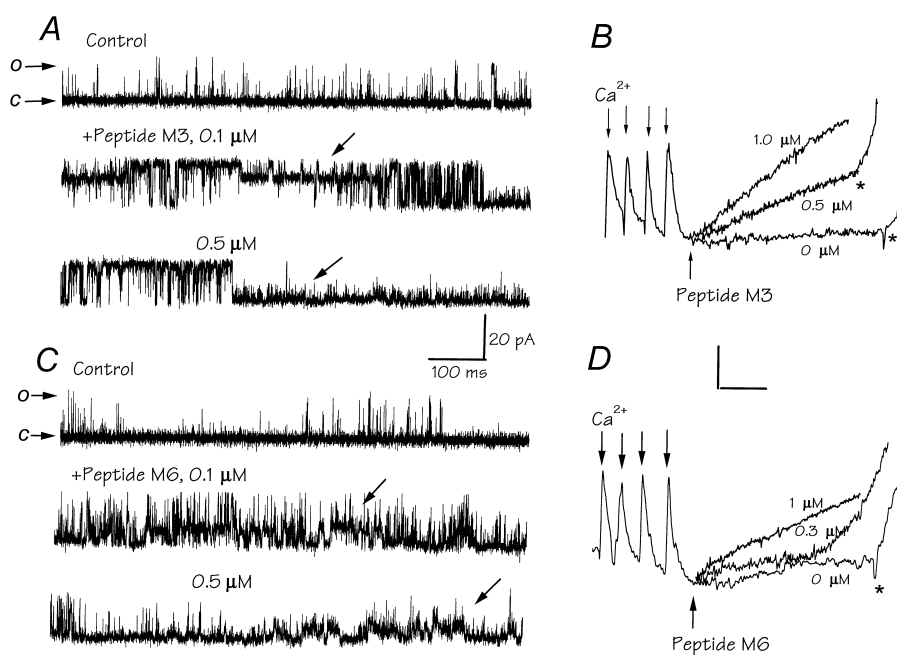

Fig. 3. The functional effect of peptides M3 and M6 on RyR1. Rabbit RyR1 channels were reconstituted in planar lipid bilayers [14,16] and activated by 10 μM (*cis*) cytosolic Ca^{2+} in the absence ('control') and ∼1 min after addition of indicated concentrations of peptide M3 (A) or peptide M6 (C) to the *cis* side. The peptides induced the appearance of subconductance states of a long lifetime (arrows). Holding potential: −35 mV for all traces. c = closed, o = open. Ca^{2+} release from actively loaded SR vesicles by peptide M3 (B) or peptide M6 (D) was measured with the spectrophotometric Ca^{2+} indicator Antipyrylazo III, as described [16]. Arrows indicate the addition of 10 nmol of Ca^{2+} to the 1 ml reaction medium. Thapsigargin (1 μM) was added simultaneously with the peptides to block Ca^{2+} uptake by the SR. When an equilibrium was reached, the Ca^{2+} ionophore A23187 (5 μM) was added to assess the SR Ca^{2+} content (asterisks). Calibration bars: 60 s (horizontal) and 5 μM Ca^{2+} (vertical).
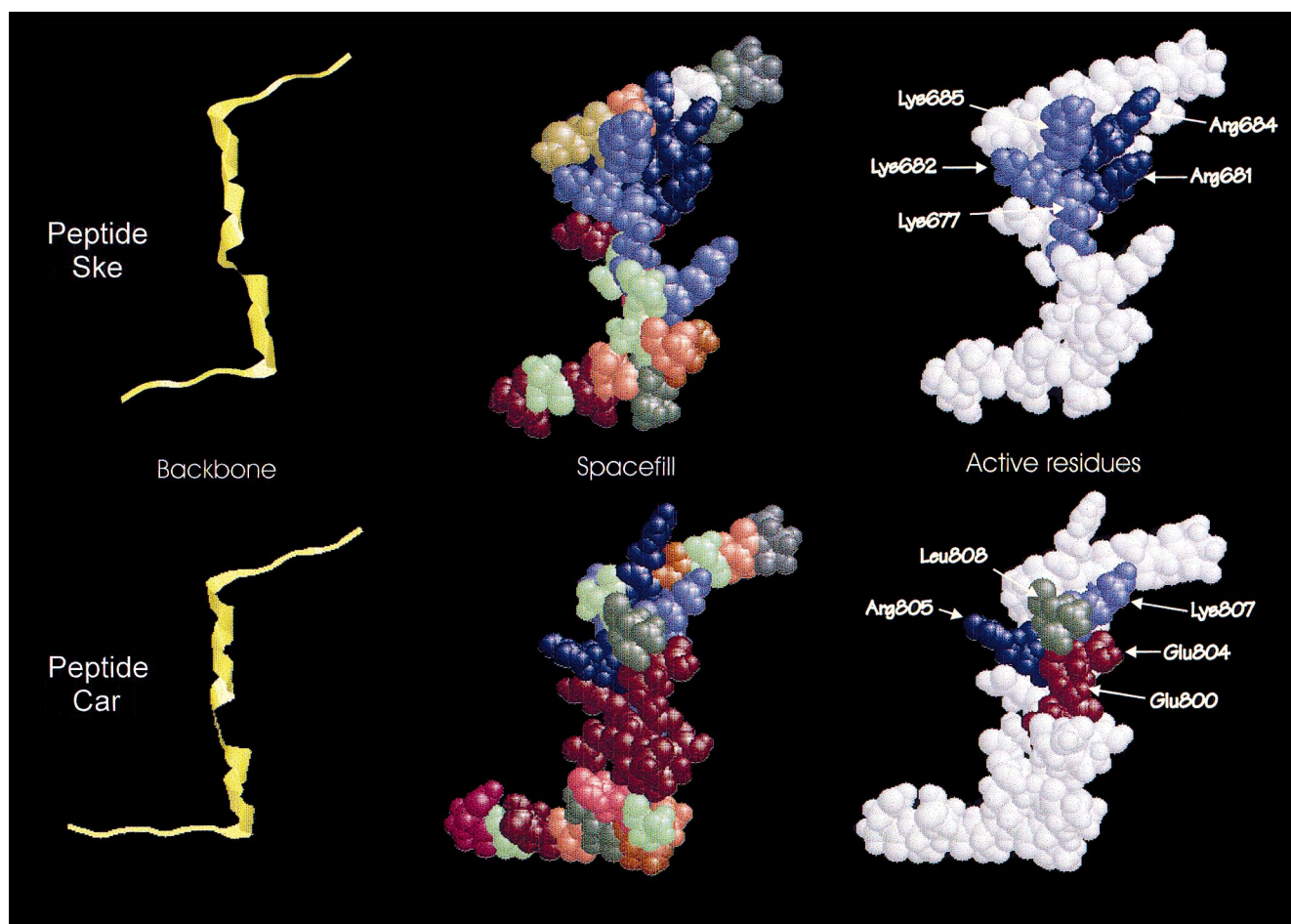
Fig. 4. Structural models of peptides Ske and Car. Backbone: the thick ribbons in the carbon backbone representation indicate regions of α-helix, while the thin threads correspond to segments of random coil. In this perspective, the top and bottom threads correspond to the carboxyl- and amino-terminal segments, respectively. The central α-helices correspond to amino acid sequences given in the text. Spacefill: the amino acid residues giving rise to the carbon backbone are shown as CPK structures. Color code: arginine, purple; lysine, blue; glutamate, red; methionine, white; alanine, light green; glutamine, pink; proline, gray; serine, orange; leucine, dark green. Active residues: the amino acid residues forming the putative structural domain that binds to RyRs are shown in color. Residues in white correspond to inactive residues, with the exception of Ser[687] of peptide Ske, which in other studies [16,17] has been shown to modulate the activity of RyRs.

these negatively charged residues is the fact that peptides M1, M2, CT, M4 and M5, which contain Glu[800] or Glu[804] (Fig. 1A), were incapable of activating [^{3}H]ryanodine binding (Fig. 2). The most dramatic example was peptide M5, which was turned into an active peptide (peptide M6) only after removal of Glu[800]. The model may also explain why the truncated peptide M3, while endowed with a minimal activatory sequence (the cluster of basic residues of region 2 [19]), was less effective than the whole peptide Ske to activate RyRs despite the absence of Glu[800] and Glu[804]. A plausible explanation is that peptide M3 lacks the positive electrical charge corresponding to Lys[677] of peptide Ske. The role of Leu[808] of peptide Car (which appears in place of Lys[685] of peptide Ske) is uncertain because we did not mutate this residue.

In summary, our results with synthetic peptides corresponding to defined segments of the II-III loop identify specific amino acids indispensable for activation of RyRs and those unfavorable for the binding of the active domain. In peptide Ske, Arg[681], Lys[682], Arg[684] and Lys[685] within the cluster of basic residues of region 2 appear as essential components of the active domain, with Lys[677] of region 1 playing a complementary role. The high electrostatic potential created by this conglomerate of positive electrical charges is absent in peptide Car which, in fact, displays some features that are counterproductive for activation of RyRs, such as the presence of Glu[800] and Glu[804]. Although the participation in E-C coupling of the segment of the II-III loop studied here has been challenged [20] and awaits further testing, our results provide a structural framework for a mechanical model in which specific amino acids of the II-III loop are capable of interacting with RyRs and triggering Ca^{2+} release.

References

[1] Endo, M. (1977) Physiol. Rev. 57, 71–108.
[2] Fabiato, A. (1985) J. Gen. Physiol. 85, 291–320.
[3] Armstrong, C.M., Bezanilla, F.M. and Horowicz, P. (1972) Biochem. Biophys. Acta 267, 605–608.

[4] Chandler, W.K., Rakowski, R.F. and Schneider, M.F. (1976) J. Physiol. (London) 254, 285–316.

[5] Ríos, E. and Pizarro, G. (1992) Physiol. Rev. 71, 849–908.

[6] Tanabe, T., Beam, K.G., Adams, B.A., Niidome, T. and Numa, S. (1990) Nature, 567–569.

[7] Nakai, J., Ogura, T., Protasi, F., Franzini-Armstrong, C., Allen, P.D. and Beam, K.G. (1997) Proc. Natl. Acad. Sci. USA 94, 1019–1022.

[8] Lu, X., Xu, L. and Meissner, G. (1994) J. Biol. Chem. 269, 6511–6516.

[9] El-Hayek, R., Antoniu, B., Wong, U.I., Hamilton, S.L. and Ikemoto, N. (1995) J. Biol. Chem., 22116–22118.

[10] Meissner, G. (1984) J. Biol. Chem. 259, 2365–2374.

[11] Zamudio, F., Gurrola, G.B., Arévalo, C., Sreekumar, R., Walker, J.W., Valdivia, H.H. and Possani, L.D. (1997) FEBS Lett. 405, 385–389.

[12] Muñoz, V. and Serrano, L. (1997) Biopolymers 41, 495–509.

[13] King, R.D. and Sternberg, M.J. (1996) Protein Sci. 5, 2298–2310.

[14] El-Hayek, R., Lokuta, A.J., Arévalo, C. and Valdivia, H.H. (1995) J. Biol. Chem. 270, 28696–28704.

[15] Xiao, R.-P., Valdivia, H.H., Bogdanov, K., Valdivia, C., Lakatta, E.G. and Cheng, H. (1997) Physiology 500, 343–354.

[16] Gurrola, G.B., Arévalo, C., Sreekumar, R., Lokuta, A.J., Walker, J.W. and Valdivia, H.H. (1999) J. Biol. Chem. 274, 7879–7886.

[17] Lu, X., Xu, L. and Messner, G. (1995) J. Biol. Chem. 270, 18459–18464.

[18] Yamazawa, T., Takeshima, H., Shimuta, M. and Iino, M. (1997) J. Biol. Chem. 272, 8161–8164.

[19] El-Hayek, R. and Ikemoto, N. (1998) Biochemistry 37, 7015–7020.

[20] Nakai, J., Tanabe, T., Konno, T., Adams, B. and Beam, K.G. (1998) J. Biol. Chem. 273, 24983–24986.